

T. Sailer,^{1,2} I. Arapoglou,¹ A. Egl,^{1,2} F. Heiße,¹ F. Hahne,^{1,2} M. Höcker,¹
B. Tu,¹ J. R. Crespo López-Urrutia,¹ A. Weigel,¹ R. Wolf,³ S. Sturm,¹ K. Blaum¹

¹ Max-Planck-Institut für Kernphysik, Saupfercheckweg 1, D-69117 Heidelberg

² Fakultät für Physik und Astronomie, Universität Heidelberg, D-69120 Heidelberg

³ ARC Centre of Excellence for Engineered Quantum Systems, School of Physics, The University of Sydney, NSW Australia

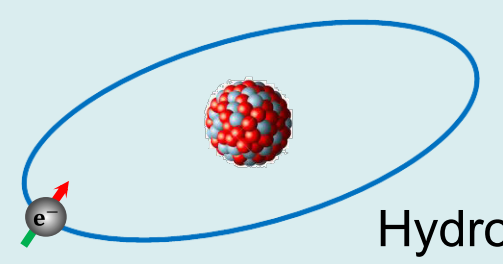
The g-factor of highly charged ions

- The g-factor of the bound electron is altered by bound-state quantum electrodynamic (BS-QED) effects

$$g = 2(1 + a_{\text{Breit}} + a_{1\text{loop}} + a_{\text{NuclearSize}} + a_{2\text{loop}} + a_{\text{recoil}} + \dots)$$

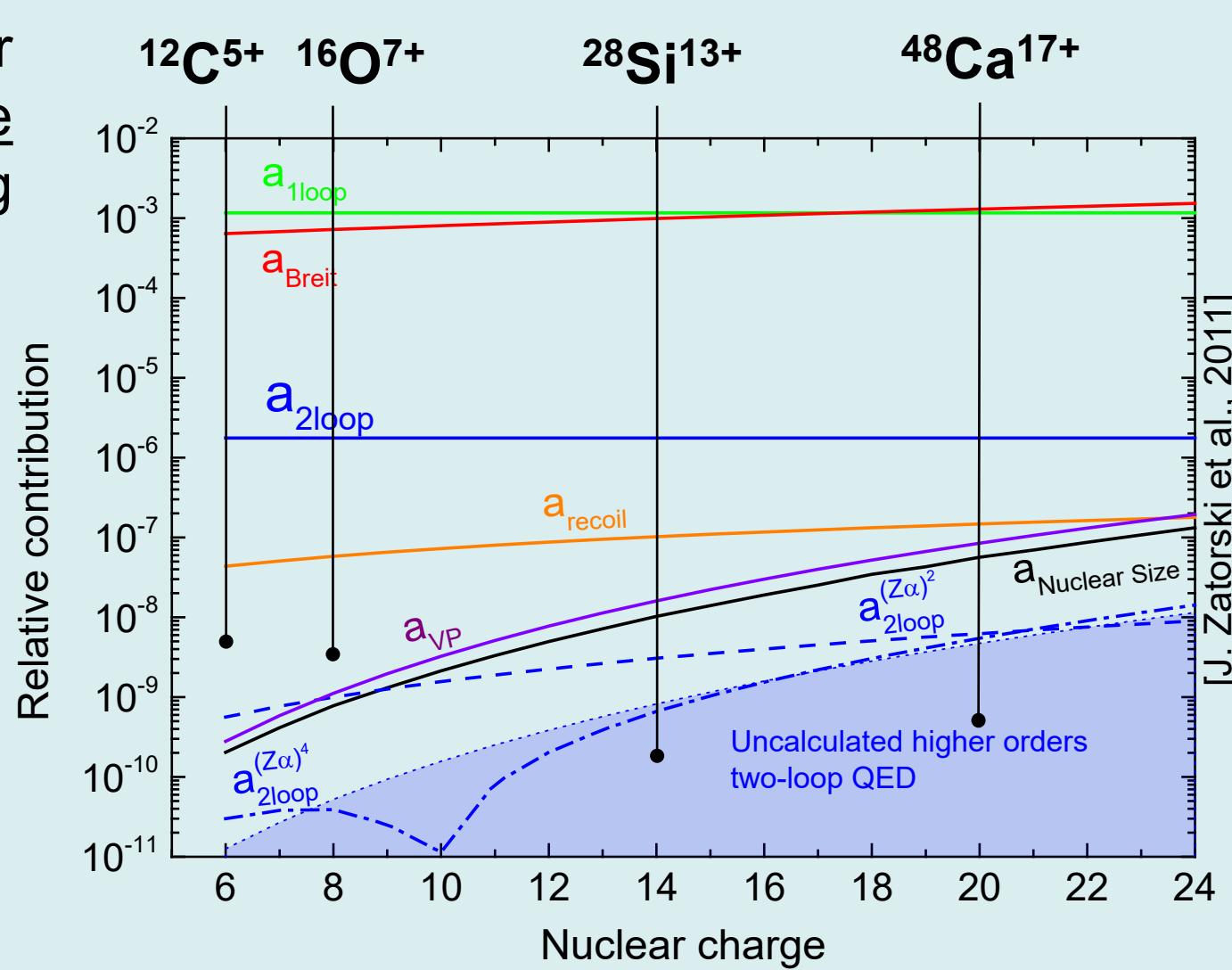
- BS-QED calculations can be tested with high-precision g-factor measurements of electrons bound in highly charged ions [1]

- BS-QED effects increase with the nuclear charge state. Therefore few or single electron systems are especially interesting (fieldstrengths up to $\sim 10^{18}$ V/m)



Hydrogen-like system

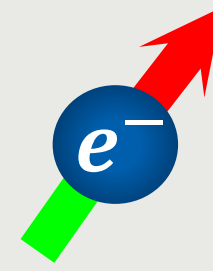
High precision measurements of $^{12}\text{C}^{5+}$, $^{16}\text{O}^{7+}$, $^{28}\text{Si}^{13+}$ and up to $^{48}\text{Ca}^{17+}$ have been performed at the Mainz g-factor experiment [2-7]



g-factor:

$$\vec{\mu}_s = -g_s \mu_B \frac{\vec{s}}{\hbar}$$

Relates the magnetic moment $\vec{\mu}_s$ to the spin \vec{s}



However, at high Z nuclear effects increase and are poorly known. **Comparison of the absolute g-factor values is therefore unfavorable** since the error will most likely be dominated by the uncertainty of the nuclear structure parameters. Instead, one can compare specific weighted g-factor differences, where nuclear effects can be canceled by a weight parameter ξ [8].

By measuring g-factor differences of **H-like** and **Li-like** ions, **QED** can be tested because nuclear contributions are highly suppressed.

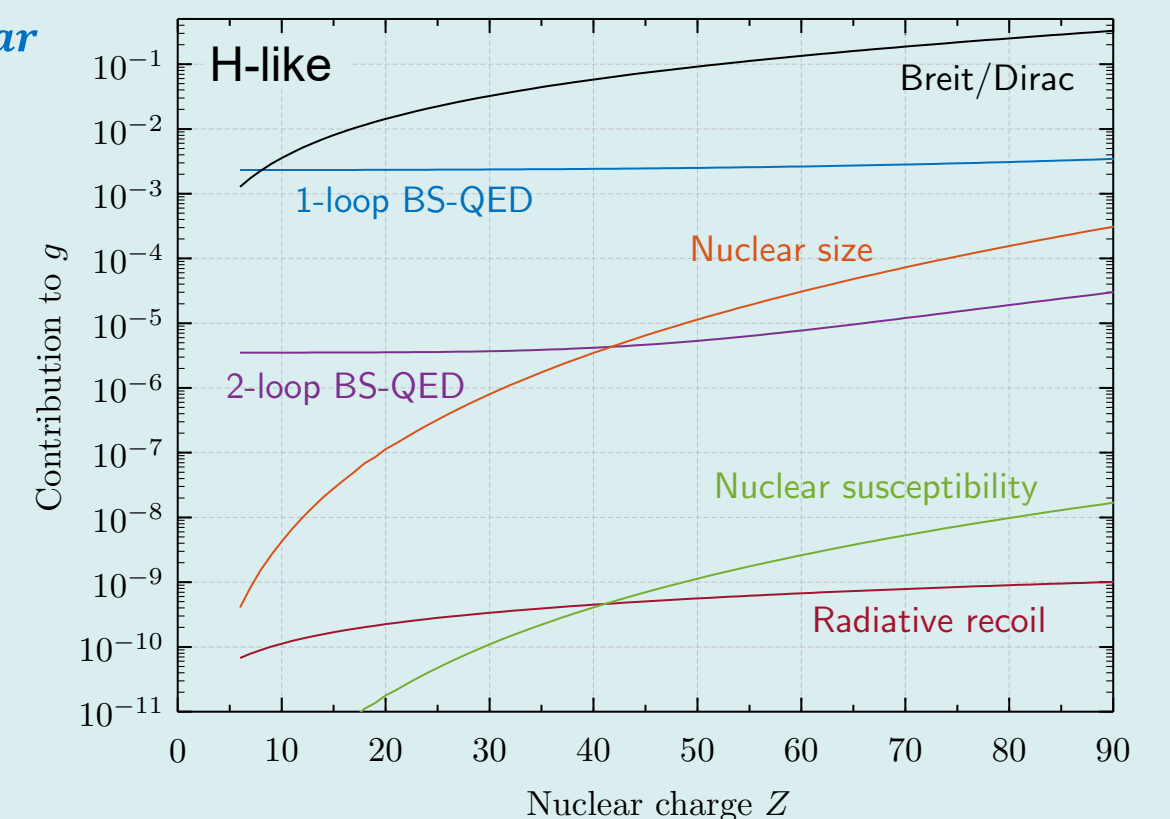
$$\Delta g' = g_{(1s)^2(2s)^2} - \xi g_{1s}$$

QED test and fundamental constants

ALPHATRAP @ MPIK - "pushing the limits"

- follow-up of the Mainz g-factor experiment
- access to Heidelberg-EBIT**
 - extend g-factor experiments to heavy-Z systems by using **heavy highly charged ions up to $^{208}\text{Pb}^{81+}$**
- probe QED in the most extreme fields, access fundamental constants

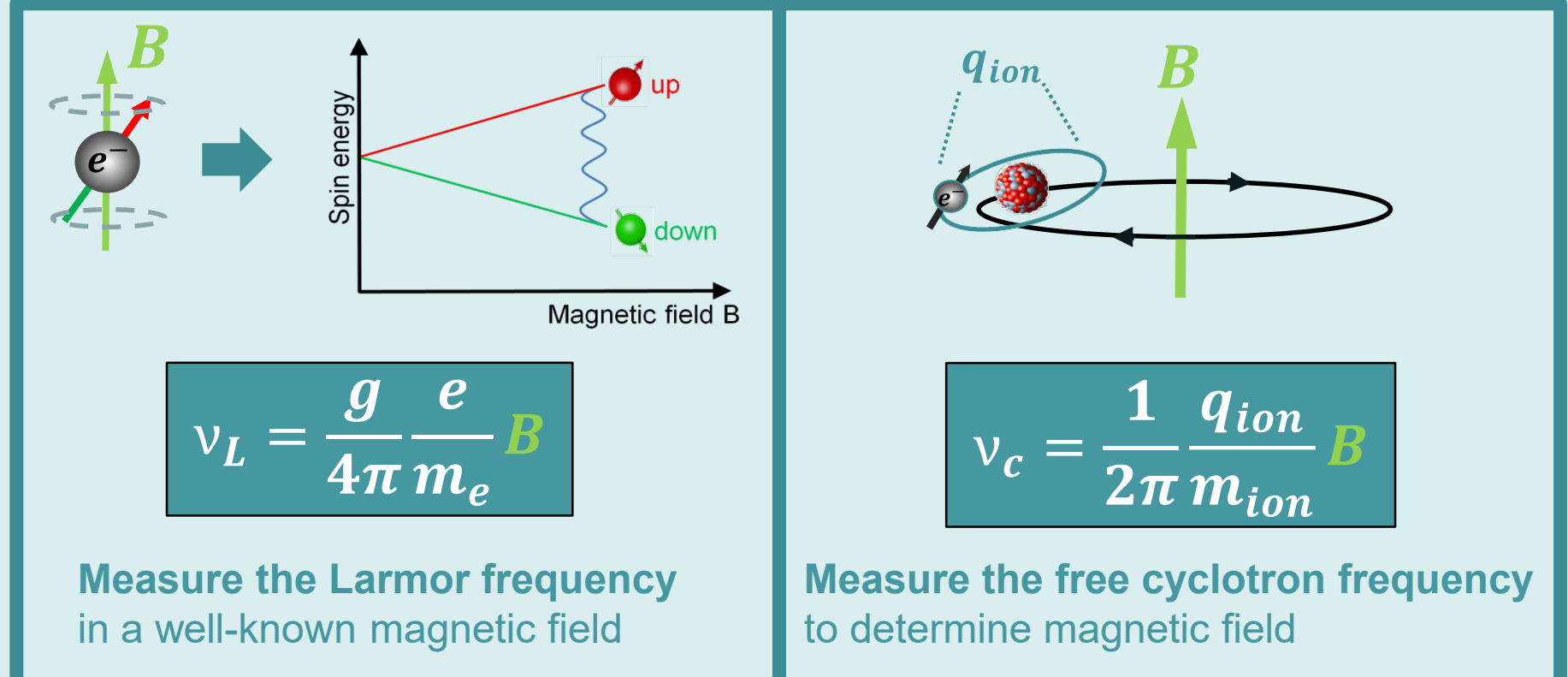
$$g = 2 + \Delta g_{\text{relat.}} + \Delta g_{\text{QED}} + \Delta g_{\text{nuclear}}$$



By measuring g-factor differences of **H-like** and **B-like** ions will allow the determination of the **fine-structure constant α** to high precision [8].

$$\Delta g' = g_{(1s)^2(2s)^2 2p_{1/2}} - \xi g_{1s}$$

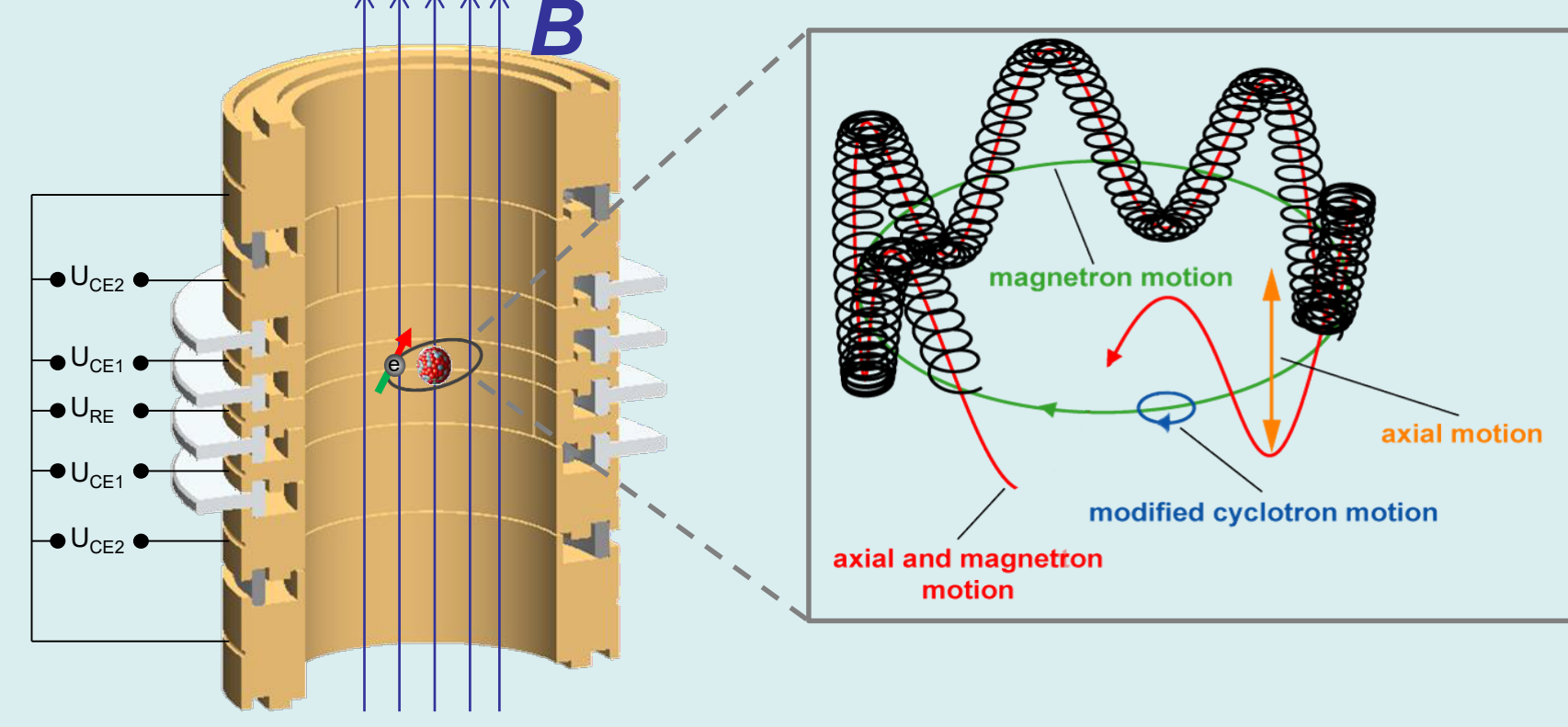
Measurement principle



$$g = 2 \left(\frac{\nu_L}{\nu_c} \right) \left(\frac{q_{\text{ion}}}{e} \right) \left(\frac{m_e}{m_{\text{ion}}} \right)$$

$\Gamma = \frac{\nu_L}{\nu_c}$ has to be measured Independent precision experiments [4,9]

Single ion in a Penning trap

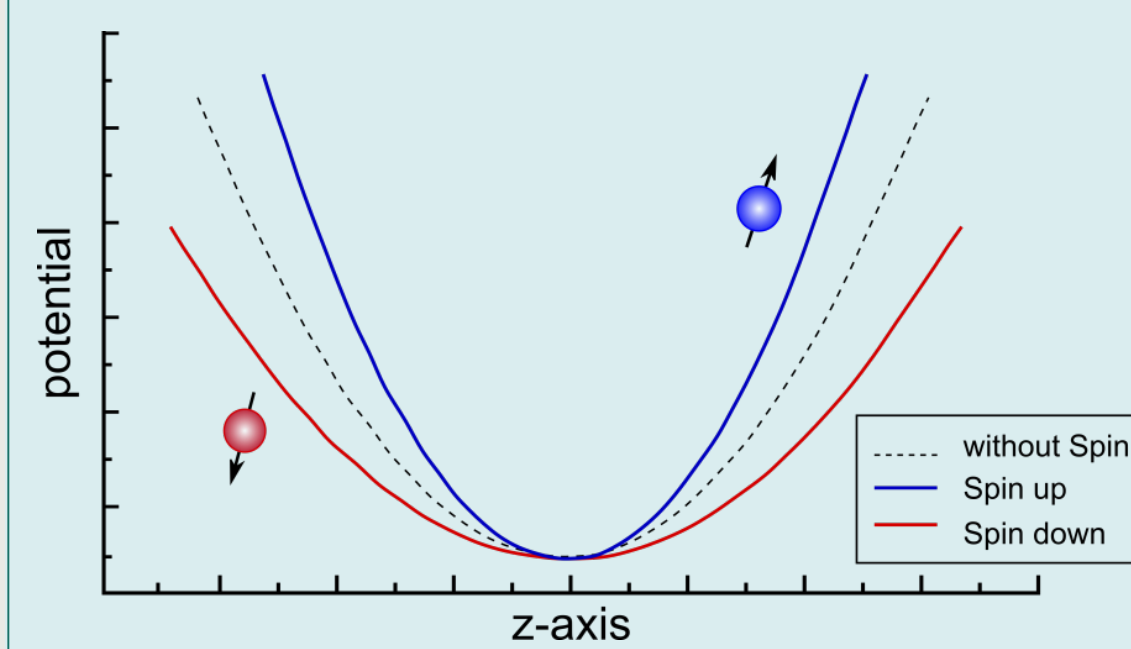
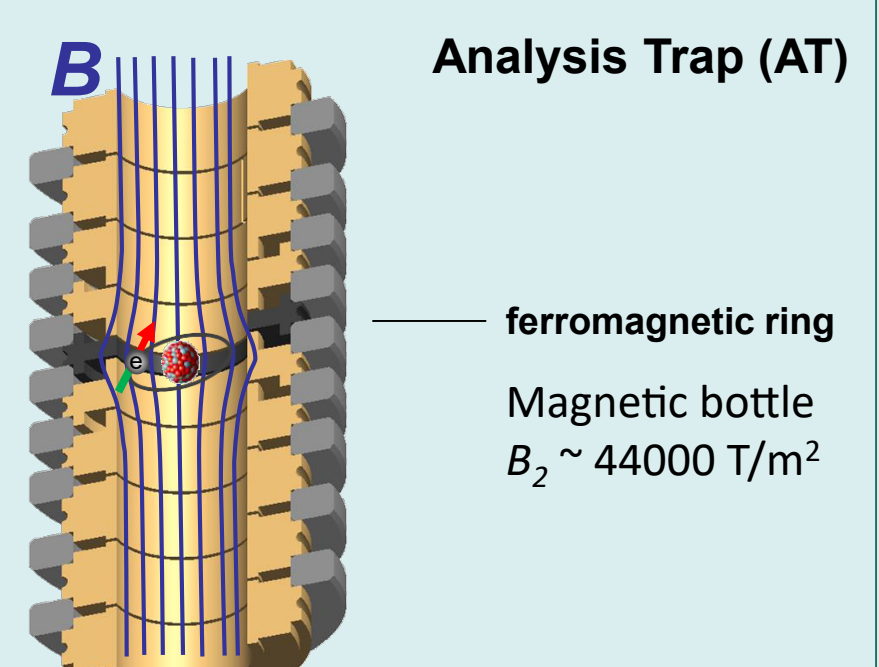


Ions can be stored in a Penning trap, which is a superposition of a strong, homogeneous magnetic field and an electrostatic quadrupolar potential. In the trap, the ions have three independent modes, where the eigenfrequencies obey the relation (invariance theorem[11]):

$$\nu_c^2 = \nu_+^2 + \nu_z^2 + \nu_-^2$$

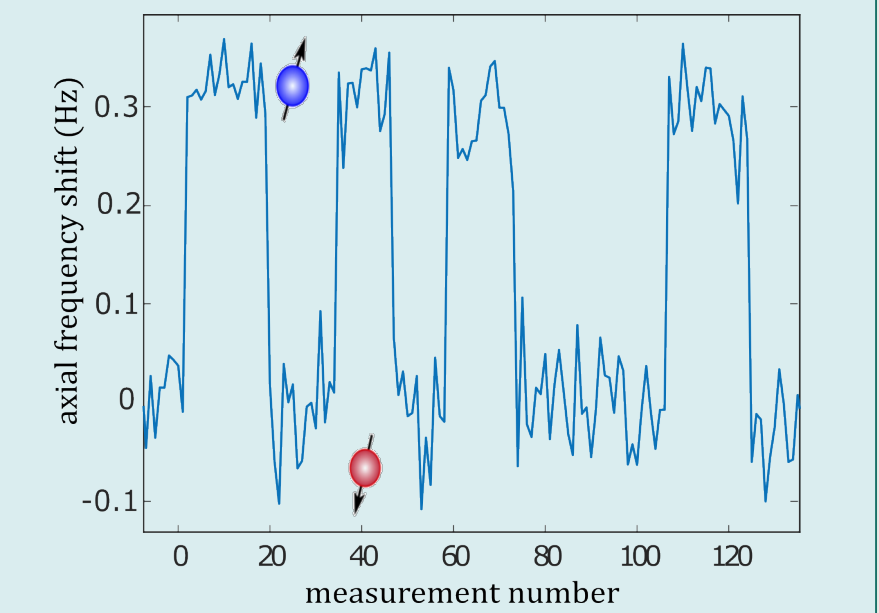
Continuous Stern-Gerlach effect

In order to detect the spin direction, a ferromagnetic ring in the analysis trap (AT) produces a magnetic field inhomogeneity (magnetic bottle), which couples the spin orientation to the axial frequency.



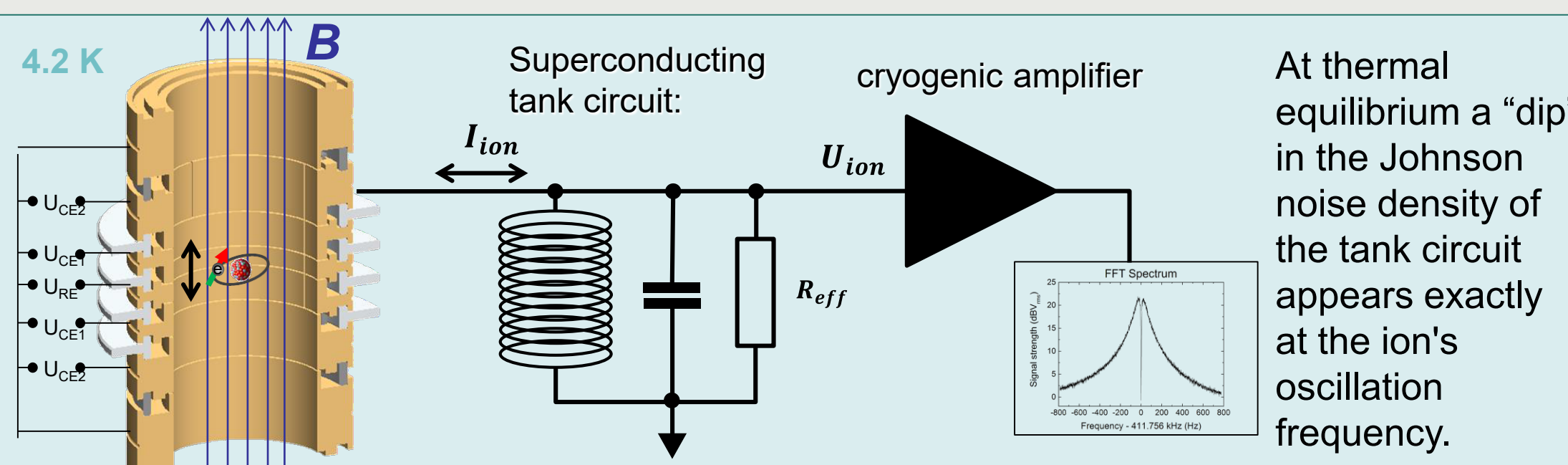
The axial potential and therefore also the axial frequency depend on the spin state of the electron. Thus, a spinflip can be observed via a change in the axial frequency given by

$$\Delta \nu_z \approx \frac{B_z g \mu_B}{4 \pi^2 m_{\text{ion}} \nu_z}$$

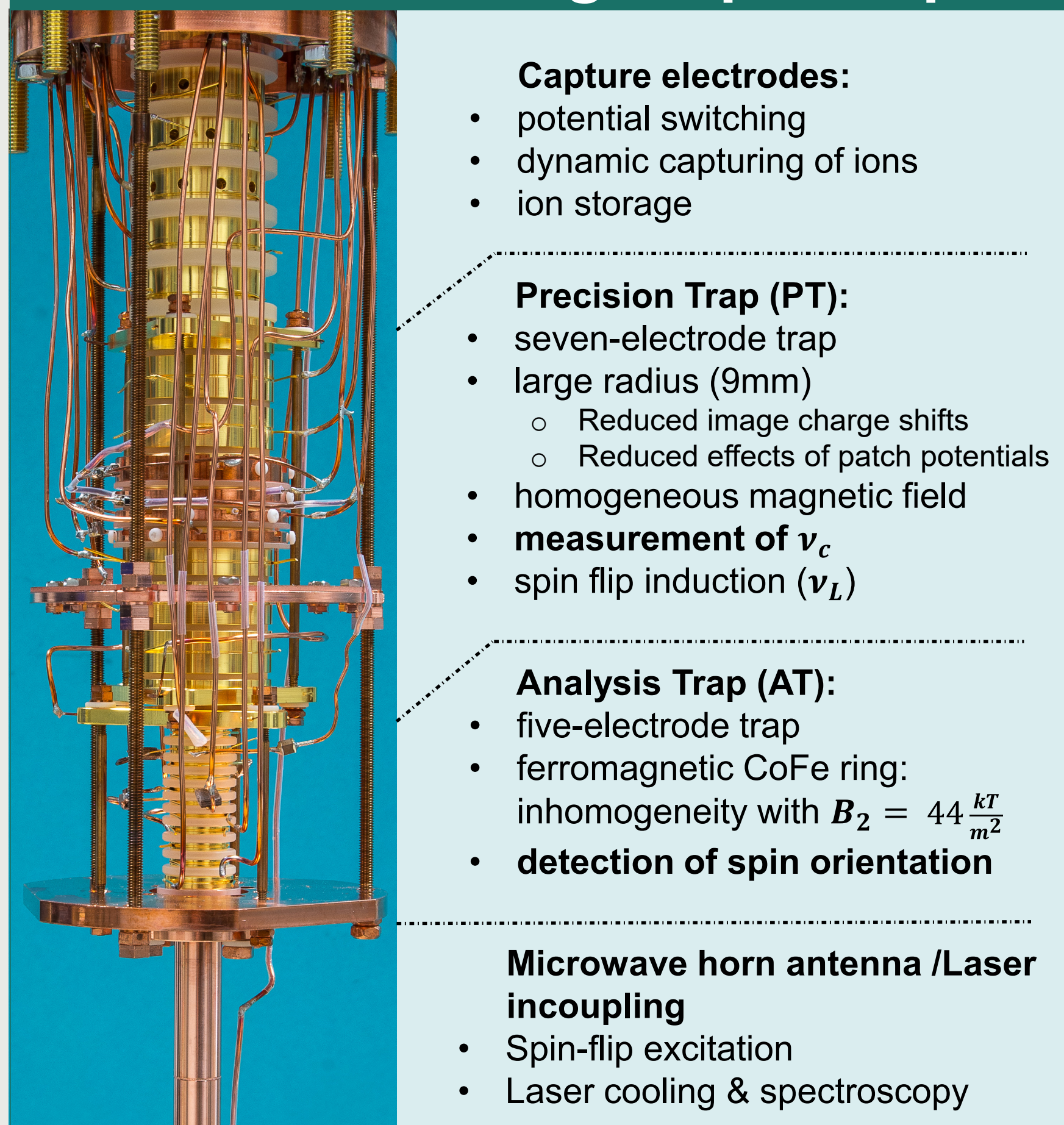


Frequency determination

The ion oscillation induces tiny image currents (\sim fA) in the trap electrodes. A superconducting high impedance tank circuit converts these currents into a measurable voltage signal. This signal is then amplified by a cryogenic low noise amplifier and can be detected frequency- or phase-resolved [12].



Double Penning trap setup



Capture electrodes:

- potential switching
- dynamic capturing of ions
- ion storage

Precision Trap (PT):

- seven-electrode trap
- large radius (9mm)
 - Reduced image charge shifts
 - Reduced effects of patch potentials
- homogeneous magnetic field
- measurement of ν_c**
- spin flip induction (ν_L)

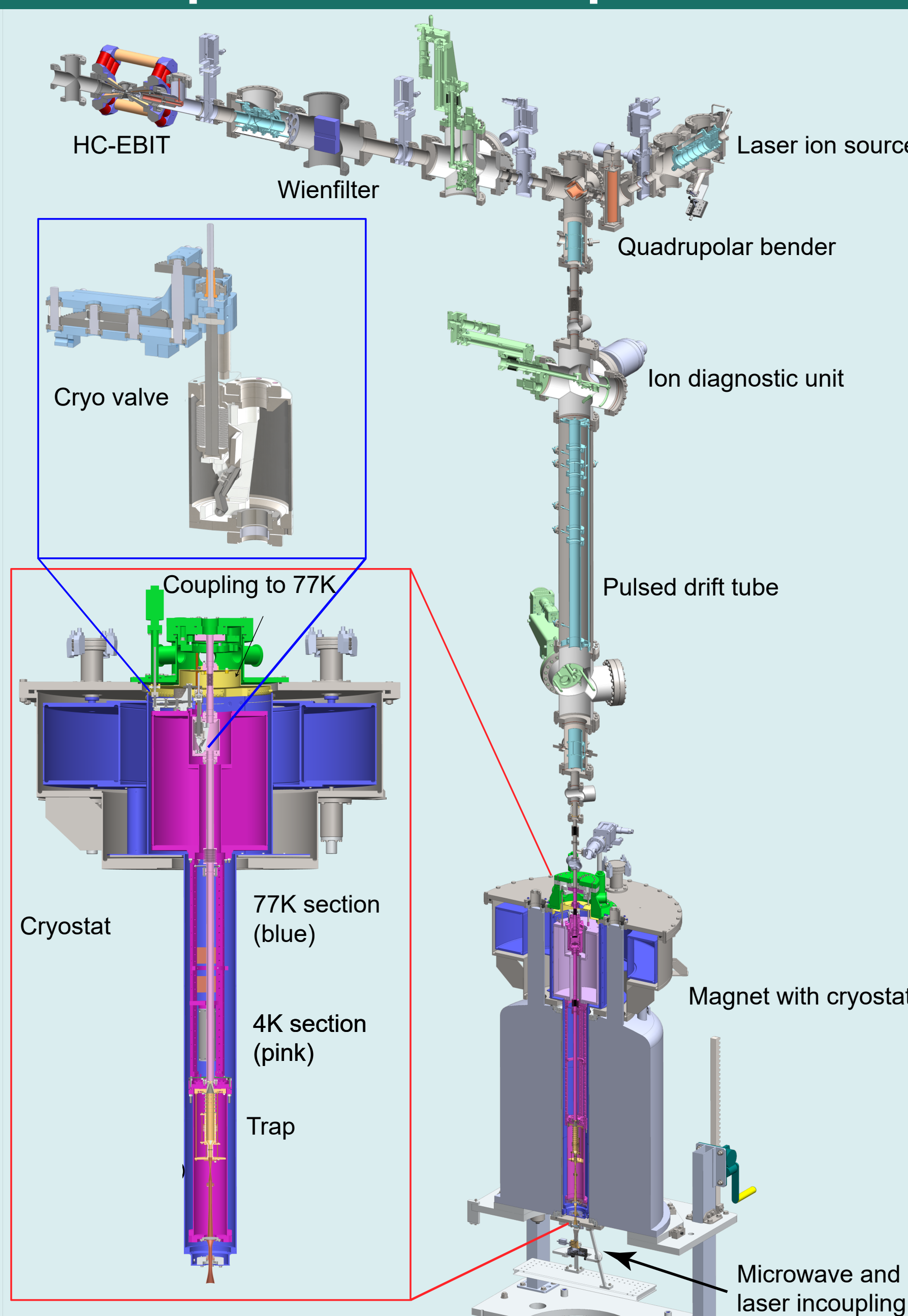
Analysis Trap (AT):

- five-electrode trap
- ferromagnetic CoFe ring: inhomogeneity with $B_z = 44 \frac{\text{K}}{\text{m}^2}$
- detection of spin orientation**

Microwave horn antenna /Laser incoupling

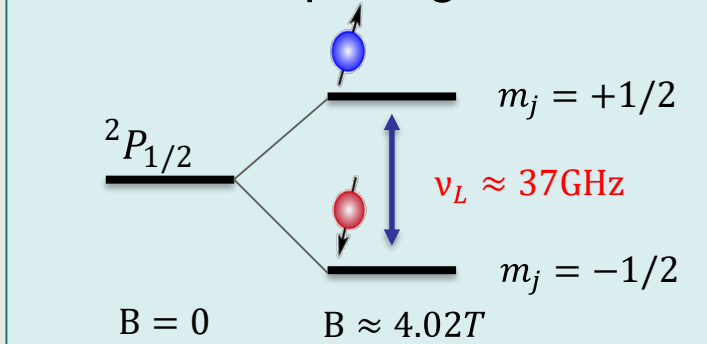
- Spin-flip excitation
- Laser cooling & spectroscopy

Experimental setup



The g-factor of boronlike argon $^{40}\text{Ar}^{13+}$

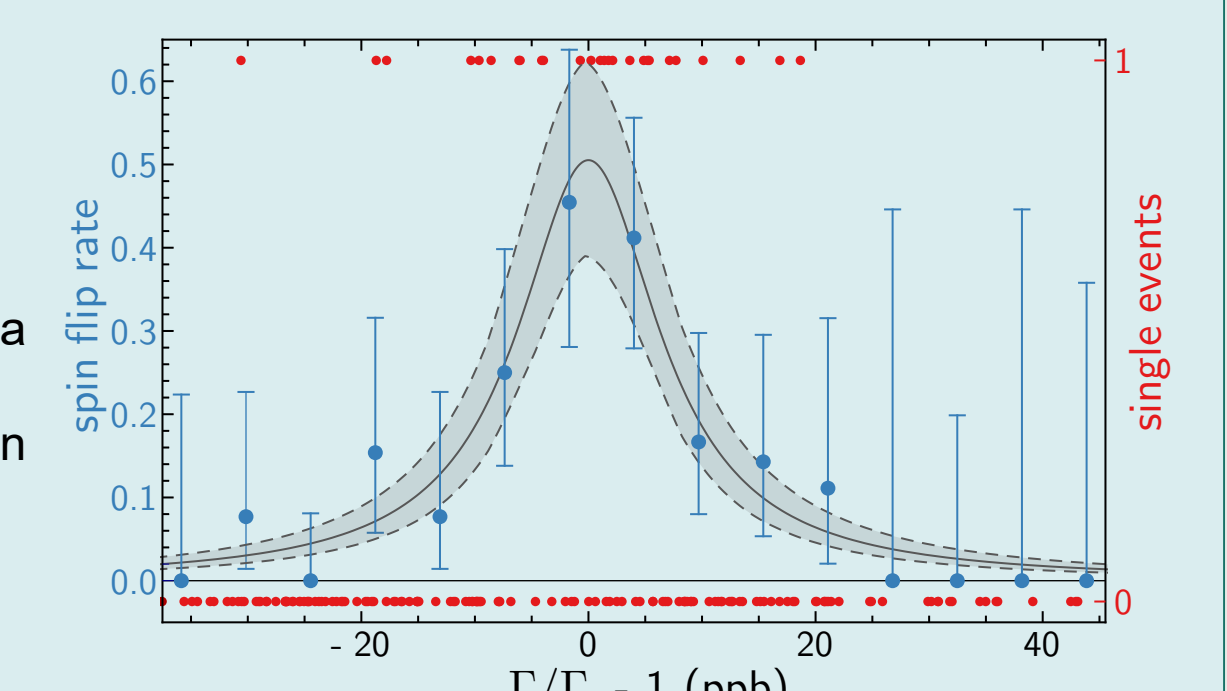
Zeeman splitting of $^{40}\text{Ar}^{13+}$



The exact Larmor frequency ν_L is determined by shining in microwaves around the supposed Larmor frequency. At ν_L the spinflip probability is maximized.

Probing the Zeeman transition multiple times for different Γ -ratios a resonance appears from which the g-factor is extracted by a Lorentzian most likelihood fit.

$$g = 2 \Gamma \frac{q_{\text{ion}}}{e} \frac{m_e}{m_{\text{ion}}} \quad \Gamma = \frac{\nu_L}{\nu_c}$$



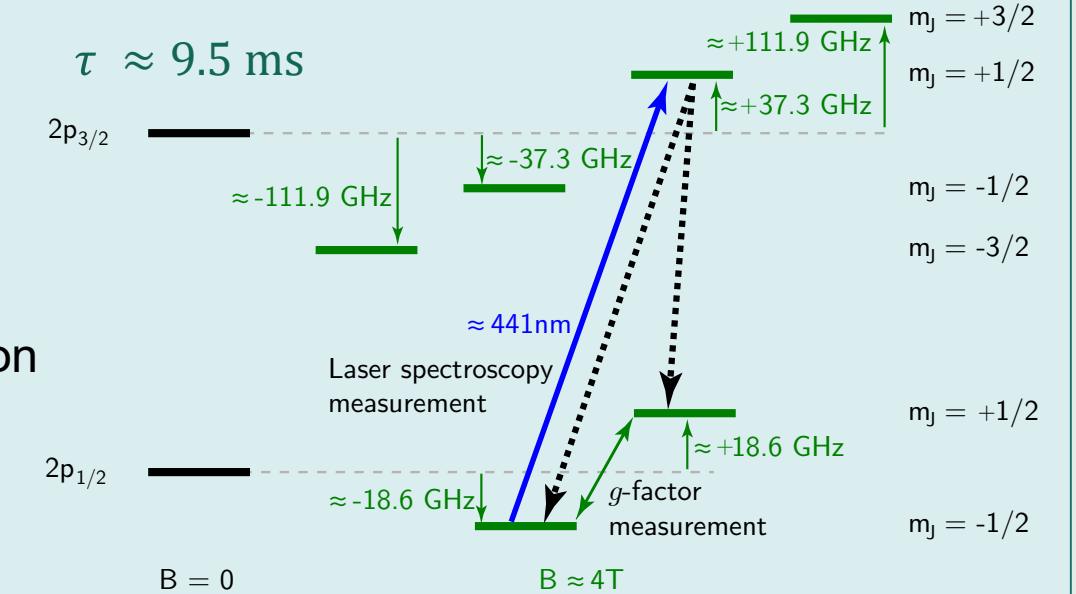
Our experimental result is in agreement with the current theory at 10^{-7} level. **Experiment precision at 10^{-9}**

Laser spectroscopy of $^{40}\text{Ar}^{13+}$

The development of a new measurement technique [17] combining laser spectroscopy with the continuous Stern-Gerlach effect (CSGE) allows precision spectroscopy on narrow transitions, being **independent** of fluorescent detection.

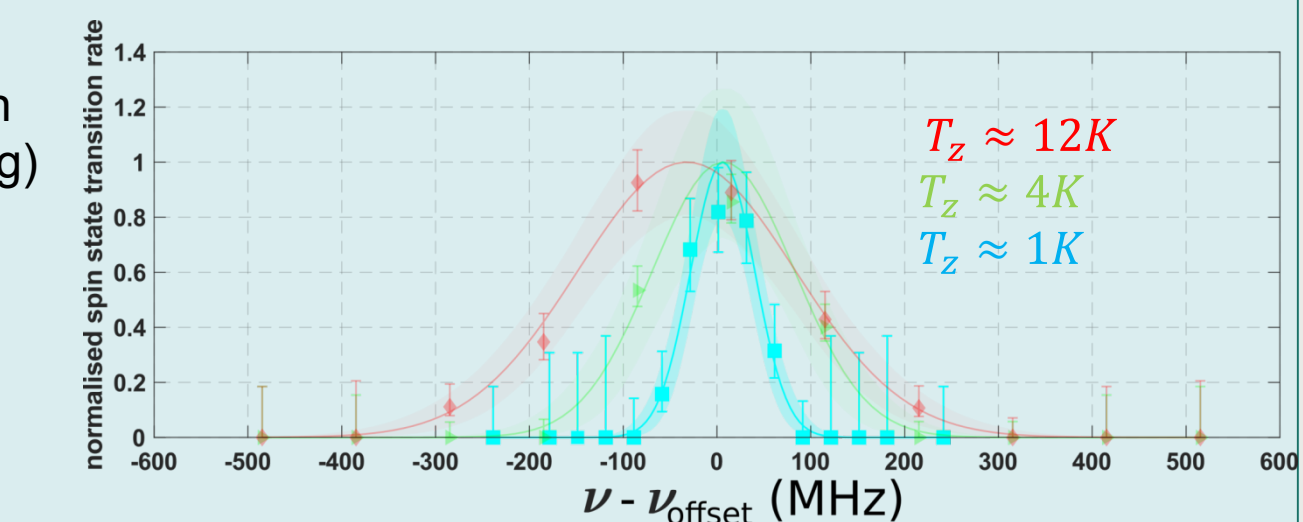
Fine structure spectroscopy in $^{40}\text{Ar}^{13+}$:

- Ion is prepared in "spin down" state
- Laser excitation near **441nm transition**
- Spontaneous decay to dark state with "spin up" indicates successful excitation
- Spin state is analyzed with CSGE



Linewidth dependent on axial ion temperature (Doppler broadening)

$$\Delta \nu_{\text{FWHM}} = \nu_0 \sqrt{\frac{8 k_B T \ln(2)}{m_{\text{ion}} c^2}}$$



References

- [1] G. Werth et al., Int. J. Mass Spectrom. 152 (2006)
- [2] H. Häfner et al., Phys. Rev. Lett. 85, 5308 (2000)
- [3] J. Verdú et al., Phys. Rev. Lett. 92, 093002 (2004)
- [4] S. Sturm et al., Nature 506, 467 (2014)
- [5] S. Sturm et al., J. Phys. B 42, 154021 (2010)
- [6] S. Sturm et al., Phys. Rev. Lett. 107, 023002 (2011)
- [7] F. Köhler, Nat. Commun. 7, 10246 (2016)
- [8] V. Shabaev et al., PRL 96, 253002 (2006)
- [9] G. Audi et al., Chinese Phys. C36, 1287 (2012)
- [10] A. Wagner et al., PRL 110, 033003 (2013)
- [11] L. S. Brown & G. Gabrielse, Rev. Mod. Phys. 58(1), 233 (1986)
- [12] S. Sturm et al., Phys. Rev. Lett. 107, 143003 (2011)
- [13] A. A. Shchepetov et al., J. Phys. Conf. Ser. 583 012001 (2015)
- [14] J. P. Marques et al., Phys. Rev. A 94, 042504 (2016)
- [15] V. A. Agababov et al., J. Phys. Conf. Ser. 1138, 012003 (2018)
- [16] I. Arapoglou et al., Phys. Rev. Lett. 122, 253001 (2019)
- [17] A. Egl et al., Phys. Rev. Lett. 123, 123001 (2019)



Acknowledgements

This work was supported by the Max-Planck Society, the IMPRS-QD, the DFG (SFB 1225- ISOQUANT) and the EU (ERC Grant No. 290870 - MEFUCO).

Further information:

www.mpi-hd.mpg.de/blaum

